Identification of ubiquitin-proteasome system components affecting the degradation of the transcription factor Pap1

Luis Marte[a,1], Susanna Boronat[a,1], Sarela García-Santamarina[a,2], José Ayté[a], Kenji Kitamura[b], Elena Hidalgo[a,*]

[a] *Oxidative Stress and Cell Cycle Group, Universitat Pompeu Fabra, C/ Doctor Aiguader 88, 08003, Barcelona, Spain*
[b] *Center for Gene Science, Hiroshima University, 1-4-2 Kagamiyama, Higashi-Hiroshima, 739-8527, Japan*

ARTICLE INFO

ABSTRACT

Signaling cascades respond to specific inputs, but also require active interventions to be maintained in their basal/inactive levels in the absence of the activating signal(s). In a screen to search for protein quality control components required for wild-type tolerance to oxidative stress in fission yeast, we have isolated eight gene deletions conferring resistance not only to H_2O_2 but also to caffeine. We show that dual resistance acquisition is totally or partially dependent on the transcription factor Pap1. Some gene products, such as the ribosomal-ubiquitin fusion protein Ubi1, the E2 conjugating enzyme Ubc2 or the E3 ligase Ubr1, participate in basal ubiquitin labeling of Pap1, and others, such as Rpt4, are non-essential constituents of the proteasome. We demonstrate here that basal nucleo-cytoplasmic shuttling of Pap1, occurring even in the absence of stress, is sufficient for the interaction of the transcription factor with nuclear Ubr1, and we identify a 30 amino acids peptide in Pap1 as the degron for this important E3 ligase. The isolated gene deletions increase only moderately the concentration of the transcription factor, but it is sufficient to enhance basal tolerance to stress, probably by disturbing the inactive stage of this signaling cascade.

1. Introduction

Aerobic organisms maintain the balance between synthesis and scavenging of reactive oxygen species such as hydrogen peroxide (H_2O_2) to reach physiological levels. When unbalances in the generation and degradation occur, oxidative stress arises and can induce toxicity due to protein, lipid or DNA oxidation [1–4]. However, cells express signaling cascades to promote cell adaptation and survival in front of enhanced steady-state levels of H_2O_2 [5–7]. These cascades normally are non-essential for viability, and mutants lacking components of the pathways do not generally display phenotypes unless oxidative stress is applied. However, tight mechanisms have to ensure that the pathways are turned on only upon stress imposition, and switched off when peroxide levels are back to normal: constitutive activation of the cascades is often deleterious for growth [8,9].

Signaling cascades, which normally have transcription factors as downstream effectors, aim at combating stress by decreasing the levels of the stress signal (i.e. through over-expression of catalases or peroxidases) and by repairing the exerted damage (i.e. by enhancing the concentration of heat shock proteins to handle oxidized/unfolded proteins, or DNA repair enzymes) [10]. Hundreds of genes are up regulated in response to environmental stresses in fission yeast to mediate cell adaptation or survival [11,12], but little is known about the effect of many of their gene products in the response to stress.

Protein oxidation is one of the toxicity hallmarks of oxidative stress [13]. Among irreversible protein modifications, protein carbonyl formation has been linked to damage and death, since it cannot be repaired and can lead to protein loss-of-function and to the formation of protein aggregates [14,15]. Protein carbonyl formation is the irreversible introduction of carbonyl groups, such as ketones, aldehydes, and lactams, on polypeptide chains. Carbonyl groups may be introduced within the protein structure at different sites and by different

mechanisms [16]. The fate of those oxidative damaged proteins that cannot be repaired is relevant in physiology and pathology, since accumulation of those species has been associated to aging and to disease [17]. In general, the proper conformation of proteins is continuously challenged by the intrinsic properties of each protein and by extrinsic factors, such as oxidative stress, which enhance the amount of protein carbonyls. Under physiological or proteostasis-efficient conditions, the protein quality control (PQC) system will try to: (i) contribute to proper protein folding during ribosomal protein synthesis; (ii) promote the reversal from misfolded states to the native protein forms; or (iii) force their degradation [18,19]. The main components of the PQC system are chaperones and degradation pathways [ubiquitin-proteasome system (UPS), and autophagy linked to the lysosome in animal cells or vacuole in yeast and plants] [20,21].

With the aim of identifying factors contributing to the removal of carbonylated proteins and, therefore, to cell adaptation to oxidative stress, we have performed a biochemical screen of ~74 *Schizosaccharomyces pombe* deletion mutants which gene products are components of the PQC system, such as members of the unfolded protein response, the UPS [E2 conjugating enzymes, E3 ligases, ubiquitin (Ub), proteasome components, deubiquitinases, chaperones]... By comparing basal and H_2O_2–induced protein carbonylation levels in extracts from these PQC mutants with those of wild-type cells, we tried to identify pathways participating in the degradation of terminally oxidized proteins. Eight of those mutants display reduced accumulation of protein carbonylation upon H_2O_2 exposure, and enhanced tolerance to peroxides. Unexpectedly, these mutants did not directly affect protein carbonyl homeostasis, but rather caused enhanced H_2O_2 scavenging through the activation of the antioxidant Pap1 signaling cascade. Thus, the eight gene mutations seem to enhance the basal level of activity of Pap1, a transcription factor known to regulate an antioxidant and pleiotropic antidrug cellular response [22,23]. Very modest upregulation of the steady-state levels of the transcription factor is sufficient to enhance the basal activity of the antioxidant cascade and to perturb wild-type tolerance to stress. We demonstrate how critical the UPS system is to regulate the concentration of transcription factors, and to maintain signal transduction cascades inactive prior to stress imposition.

2. Results

2.1. Identification of PQC-related gene deletions improving S. pombe tolerance to oxidative stress

With the aim of identifying pathways affecting the fate of irreversibly oxidized proteins, we monitored basal and H_2O_2-induced total protein carbonylation in wild-type cells and in 74 deletion mutants lacking individual PQC components (Table S1). Among them, eight mutants which gene products belong to the UPS display a total or partial reduction of protein carbonylation levels after peroxide stress (Fig. 1A): cells lacking the ribosomal-Ub fusion protein Ubi1, the Ub-conjugating E2 enzyme Ubc2/Rhp6, the Ub E3 ligases Ubr1, Hul5, Ltn1 and SPBC14F5.10c, the proteasome assembly chaperone Nas6 and the 19S proteasome base subunit Rpt4.

The lack of accumulation of oxidized proteins upon H_2O_2 stress in the mutants could be beneficial for oxidative stress survival. Therefore, we monitored the growth of wild type and mutant cell cultures in the presence or absence of peroxides. As shown in Fig. 1B, addition of 1 mM H_2O_2 to YE cultures of wild-type cells causes growth inhibition which lasts ~9 h before growth resumption. Some of the deletion mutants, such as Δ*ubi1*, Δ*ubc2*, Δ*ubr1*, Δ*hul5* or Δ*SPBC14F5.c10*, display growth defects in the absence of stress, and either do not reach the maximum OD_{600} or have longer duplication times, as reflected by the less steep slopes (Fig. 1B; see Δ*ubi1* or Δ*ubc2* as examples). In most deletion mutants, however, the lag time in the presence of peroxides is shorter than in wild-type cells, ranging from 3 to 8 h after 1 mM H_2O_2

stress (Fig. 1C). The only exception is strain Δ*ubi1*, with longer lag time than wild type cells: probably this strain has pleiotropic defects due to the general decrease in Ub levels. This confirms that the identified UPS mutants are better suited to survive in front of oxidative stress than wild-type cells.

2.2. The pap1 gene is a suppressor of the enhanced oxidative stress tolerance of the UPS gene deletions

The improved tolerance to peroxides of these UPS mutants could arise from a more efficient elimination of oxidized proteins, but also from a basal pre-activation of anti-oxidant stress pathways. *S. pombe* activates different signaling cascades depending on the extracellular H_2O_2 levels, the main ones being the Pap1 and the Sty1 pathways [for a review, see Ref. [24]]. Both pathways are essential for cell survival under conditions of oxidative stress, but mutants lacking Pap1 or Sty1 do not display strong phenotypes under basal conditions.

In particular, the transcription factor Pap1, which becomes indirectly activated by moderate peroxide levels in a peroxiredoxin Tpx1-dependent manner, accumulates in the nucleus only after stress imposition (Fig. 2A). Activation of Pap1-dependent antioxidant genes by H_2O_2 is essential to confer wild-type tolerance to the oxidant, but Pap1 was first isolated in screenings searching for mutants resistant to structurally unrelated drugs, such as brefeldin A, staurosporine or caffeine [25–27], since antioxidant signaling cascades are often associated to tolerance to multidrugs. Indeed, expression of the ABC-type transporters Hba2 and Caf5 is dependent on the transcription factor Pap1, and these efflux pumps are probably acting to extrude caffeine and other drugs from the intracellular compartment [28] (Fig. 2A). Mutations in several genes leading to constitutive activation of Pap1 have been described to enhance multidrug resistance, and two of them coincide with some of the eight mutants isolated in our oxidative stress screen: Δ*ubr1* and Δ*ubc2* [29,30]. Therefore, we decided to test whether some or all of our mutants were connected to the Pap1 pathway by analyzing first their tolerance to caffeine on solid plates. We used Δ*pap1* [28] and Δ*trr1* [27] strains as controls of impaired and enhanced caffeine resistance, respectively [in the absence of Trr1 (thioredoxin reductase) Pap1 is constitutively oxidized and active [31]]. As shown in Fig. 2B, the eight mutants isolated in our screen are resistant to caffeine on plates to the same extent as Δ*trr1*. The caffeine resistant phenotype of the UPS mutants is largely suppressed by *pap1* deletion (Fig. S1A). This would first suggest that all of them probably decrease the accumulation of protein carbonyls by an indirect mechanism, the constitutive activation of the Pap1 pathway. Second, this result also suggests that other mutants previously known to up-regulate basal Pap1 activity should also decrease the accumulation of oxidized proteins. Indeed, protein extracts from peroxide-treated Δ*trr1* cells do not contain carbonylated proteins, and in fact over-expression of the H_2O_2 scavenger catalase is sufficient to abolish protein oxidation (Fig. 2C).

To further confirm the participation of Pap1 in the enhanced tolerance to oxidative stress of our UPS mutants, we tested whether deletion of *pap1* would suppress the lack of protein carbonyls after H_2O_2 stress of the single deletion mutants. As shown in Fig. 2D, deletion of *pap1* almost totally restores wild-type levels of protein carbonyls in extracts from Δ*ubi1, Δubc2, Δubr1, Δrpt4, Δhul5* and Δ*ltn1* cells. The effect on Δ*nas6* is not clear, and *pap1* deletion only partially suppresses the phenotype of cells lacking the E3 ligase-coding gene *SPBC14F5.10c* (Fig. S1B).

Gain-of-function of Pap1 in the absence of stress can be caused by different molecular mechanisms: (i) nuclear accumulation due to genetic or drug-mediated nuclear export defects [32,33]; (ii) basal oxidation/activation of Pap1 due to genetic defects on the thioredoxin system [27,34]; and (iii) enhanced protein levels [29,30,35]. Since all our deletion mutants lack components of the UPS, we tested whether Pap1 protein levels could be increased. We tagged the endogenous *pap1* locus in the eight UPS deletion strains with *GFP*, and quantified
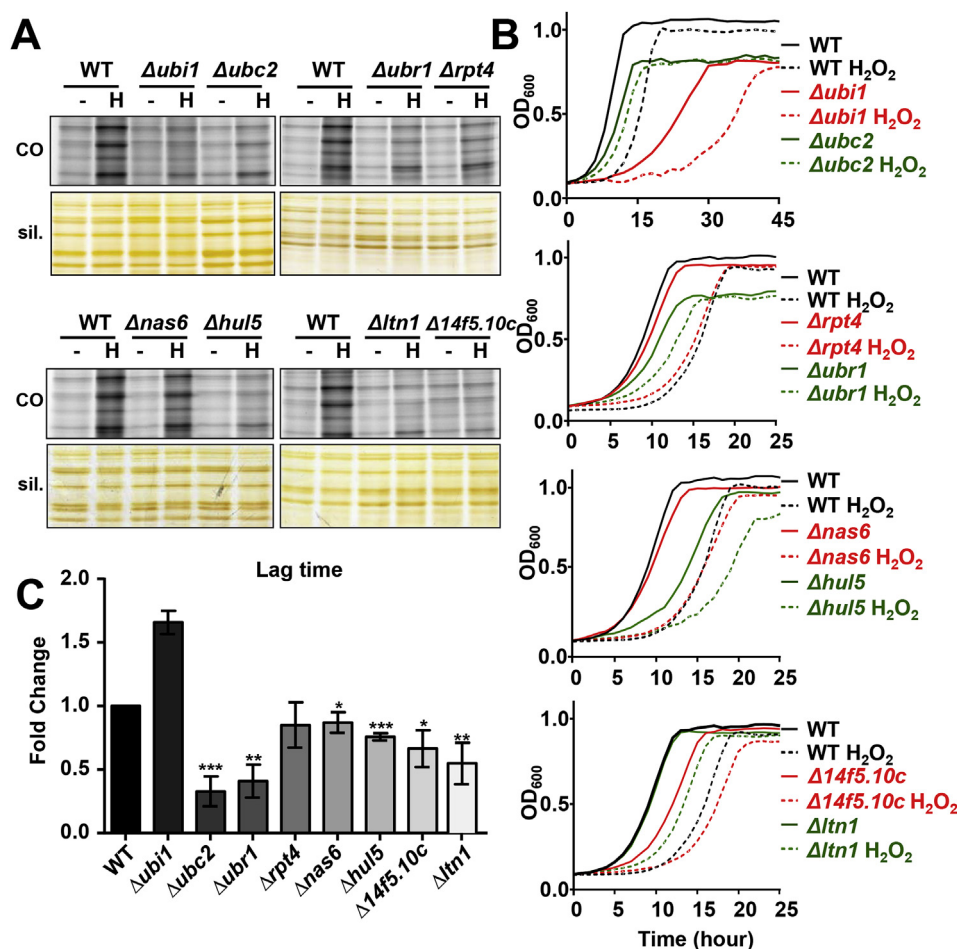
Fig. 1. Several UPS-related gene deletion mutants display high tolerance to oxidative stress. (A) Protein carbonyl determination (CO) in extracts from strains 972 (WT), SB82 (*Δubi1*), SB451 (*Δubc2*), SG282 (*Δubr1*), SB15 (*Δrpt4*), SB315 (*Δnas6*), SB22 (*Δhul5*), SB290 (*Δltn1*) and LM90 (*ΔSBPC14F5.10c*), untreated (−) or treated with 2.5 mM H_2O_2 for 4 h (H). Protein loading was assessed by silver staining (sil.). (B) Growth curves of strains described above growing in YE media with or without 1 mM H_2O_2. For each panel, representative data from at least three biological replicates is shown. (C) The time at which each strain reached half of the maximal OD_{600} was calculated from graphs in panel B for both untreated and 1 mM H_2O_2 treated cells. The lag time between treated and untreated cells to reach half of the maximal OD_{600} for each of the mutant strains described in panel B is represented as the fold change compared to the lag time for the wild-type strain which is set to 1. Data represent the average values from three biological replicates. Error bars represent SD. Statistical significance was calculated with a t-Student test with P-values of 0.05 (*), 0.01, (**) and 0.001 (***).

fluorescence levels by flow cytometry. As shown in Fig. 2E, six out of eight mutants display higher levels of Pap1-GFP than wild-type cells. We also determined untagged Pap1 protein levels in the deletion mutants by Western blot of non-native protein extracts with anti-Pap1 polyclonal antibodies, and again six out of eight mutants display higher levels that wild type cells (Fig. 2F). Only cells lacking the ribosome-linked E3 ligase Ltn1 did not display significantly higher Pap1-GFP (Fig. 2E) nor Pap1 (Fig. 2F) levels, and the lack of Ltn1 may be enhancing Pap1 basal activity by nuclear transport- or activity-based mechanisms.

2.3. The non-essential proteasome-related components Nas6 and Rpt4 participate in the maintenance of physiological low steady-state levels of Pap1

With the exception of *Δltn1*, seven UPS mutants display increased Pap1(-GFP) levels under basal conditions: cells lacking the ribosomal-Ub fusion protein Ubi1, the Ub-conjugating E2 enzyme Ubc2, the Ub E3 ligases Ubr1, Hul5, and SPBC14F5.10c, the proteasome assembly chaperone Nas6 and the 19S proteasome base subunit Rpt4. They all belong to the UPS, either at the level of Ub labeling (Ubi1, Ubc2, Ubr1, Hul5, SPBC14F5.10c) or at the proteasome level (Nas6 and Rpt4) (Fig. 3A).

Some essential components of the proteasome were soon discovered to participate in drug resistance acquisition in a Pap1-dependent manner, such as the proteasome-associated deubiquitinase Pad1 [35,36] or several *mts* subunits from the 19S or 20S proteasome [30] (Fig. 3A). We confirmed that non-specific proteasome misfunction enhances oxidative stress tolerance by measuring protein carbonylation in strains carrying some classical temperature-sensitive proteasome

alleles, such as *mts4-1, mts2-1* and *mts3-1*. As shown in Fig. 3B, even at permissive temperature (30 °C) extracts from these mutants fail to accumulate protein carbonyls after H_2O_2 treatment.

Little is known about the role of Nas6 in fission yeast, but its *S. cerevisiae* homolog is considered an important chaperone participating in proteasome assembly, providing a dual mechanism to control affinity interactions between the lid, the base and the core particle of the proteasome [37]. Therefore, it is not surprising that deletion of *nas6,* coding for a chaperone which contributes to general proteasome assembly and function, could also have a non-specific impact on Pap1 protein levels.

Regarding Rpt4, it is one of the very few non-essential proteasome subunits. It belongs to the regulatory particle, 19S, specifically to the base [38] (Fig. 3A). It has recently been linked to non-protease activities; in particular Rpt4 avoids heterochromatin spreading [39]. The fission yeast 26S proteasome is located in the inner side of the nuclear envelope during the mitotic cycle, as demonstrated by electron microscopy [40] and fluorescent microscopy [41], but the nuclear signal decreases during nitrogen starvation, probably by Crm1-mediated export of the proteasome to the cytosol [41]. We assessed by fluorescence microscopy whether GFP-Rpt4 displays a sub-cellular localization profile similar to other essential components such as the core particle subunit Pre6 or the lid deubiquitinase Pad1. As shown in Fig. 3C and Fig. S2, Pre6-GFP and Pad1-GFP have a nuclear periphery localization, which dramatically changes after nitrogen starvation, and the same behavior is observed for the GFP-Rpt4 chimera. We tested whether the proteasome also suffers localization changes under other types of nutrient starvation. Indeed, all three proteins also display re-distribution to the cytosol three days after stationary phase entry (Fig. 3D and Fig. S2). The only stress condition which seems to affect differentially Rpt4
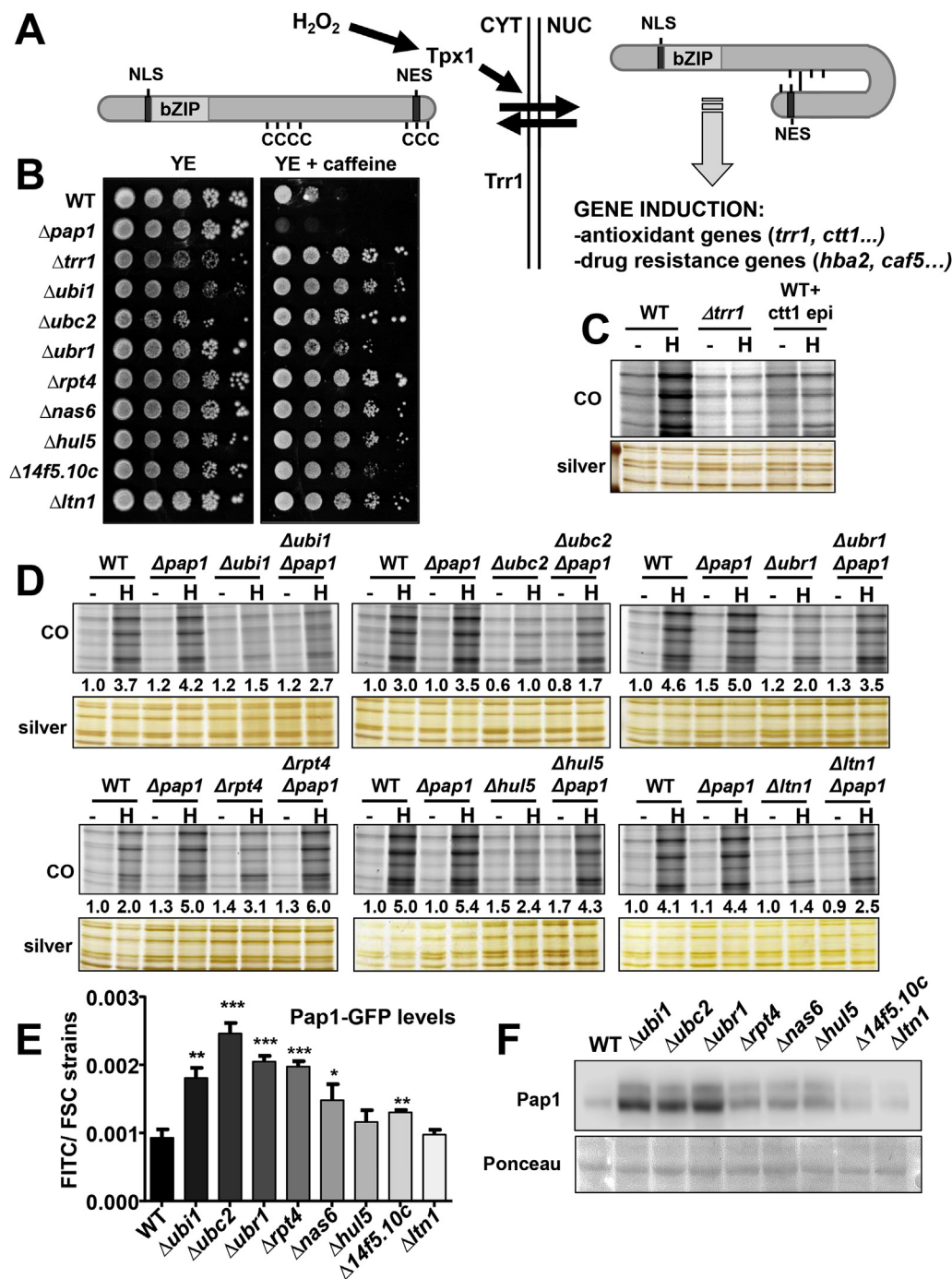
Fig. 2. Pap1 dependence of resistance to oxidative stress of UPS mutants. (A) Scheme of Pap1 activation upon mild levels of H_2O_2. (B) Resistance to caffeine of UPS mutants. 972 (WT), AV25 (Δ*pap1*), SG167 (Δ*trr1*), SB82 (Δ*ubi1*), SB451 (Δ*ubc2*), SG282 (Δ*ubr1*), SB15 (Δ*rpt4*), SB315 (Δ*nas6*), SB22 (Δ*hul5*), LM90 (Δ*SPBC14F5.10c*) and SB290 (Δ*ltn1*) cells were serially diluted and plated on YE plates containing or not 12.5 mM caffeine. (C) Protein carbonyl determination (CO) in extracts from strains 972 (WT), SG167 (Δ*trr1*) and wild-type strain HM123 transformed with episomal plasmid p419 to express *ctt1* under the control of the *sty1* promoter, untreated (−) or treated with 2.5 mM H_2O_2 for 4 h (H). Equal loading was analyzed by silver staining (silver). (D) Carbonyl protein determination (CO) of strains 972 (WT), AV25 (Δ*pap1*), SB82 (Δ*ubi1*), SG295 (Δ*ubi1* Δ*pap1*), SB451 (Δ*ubc2*), SB449 (Δ*ubc2* Δ*pap1*), SG282 (Δ*ubr1*), SG292 (Δ*ubr1* Δ*pap1*), SB15 (Δ*rpt4*), SG293 (Δ*rpt4* Δ*pap1*), SB22 (Δ*hul5*), LM39 (Δ*hul5* Δ*pap1*), SB290 (Δ*ltn1*) and LM42 (Δ*ltn1* Δ*pap1*) as described in Fig. 1. Fold induction numbers, indicated below each CO panel, are the ratio of the absolute fluorescence values and the corresponding amount of total protein, and they relate to the values of the wild-type strain (972) for each gel. (E) Steady-state Pap1-GFP levels measured by flow cytometry in cell suspensions of strains LM102 (WT), LM116 (Δ*ubi1*), LM174 (Δ*ubc2*), LM93 (Δ*ubr1*), LM99 (Δ*rpt4*), LM106 (Δ*nas6*), LM107 (Δ*hul5*), LM142 (Δ*SPBC14F5.10c*) and LM143 (Δ*ltn1*), all expressing a C-terminally GFP-tagged version of Pap1. Error bars represent SD from three biological replicates. Statistical significance was calculated with a t-Student test with P-values of 0.05 (*), 0.01, (**) and 0.001 (***). (F) Steady-state Pap1 levels determined by Western Blot of TCA extracts from strains described in Fig. 1A. Ponceau staining of membranes is used as loading control.

and other essential subunits of the proteasome, Pre6 and Pad1, is heat shock: while the Pre6 and Pad1 remain nuclear 1 h after heat-shock imposition, Rpt4 displays a dual nuclear-cytosolic localization, with apparent aggregate formation. However, oxidative stress does not alter the localization of none of the three proteasomal subunits (Fig. 3D), and we propose that the effect of Δ*rpt4* on Pap1 protein levels is due to a partial impairment of the general proteasome function.

2.4. Ubi1-Ubc2-Ubr1-dependent ubiquitin-labeling of Pap1 occurs at the nucleus even in the absence of stress

Ubr1 is a RING finger motif protein which was thought to participate in the N-end rule degradation pathway, but the homologous Ubr11 is the E3 ligase responsible of this degradation system [42]. Ubr1 has

been demonstrated to label Pap1 for degradation in the nucleus where the E3 ligase is preferentially located [29]. The lack of Ubr1, Ubc2 or Ubi1 has a direct effect on Pap1 steady-state levels, suggesting that Ub-mediated degradation of the transcription factor occurs during unstressed conditions (Fig. 4A). Pap1 displays apparent cytosolic localization prior to stress imposition, and it quickly accumulates at the nucleus after the addition of H_2O_2 in an importin Imp1-and disulfide bond-dependent manner [43–45]. Under non-stress conditions, the export of Pap1, mediated by the exportin Crm1, prevails over the import, but there is continuous shuttling of the transcription factor through the nuclear pore complex under unstressed conditions, as demonstrated by the H_2O_2-independent nuclear accumulation of Pap1 upon addition of the Crm1 inhibitor leptomycin B [33]. This shuttling may explain how the transcription factor is subject to Ubr1-dependent
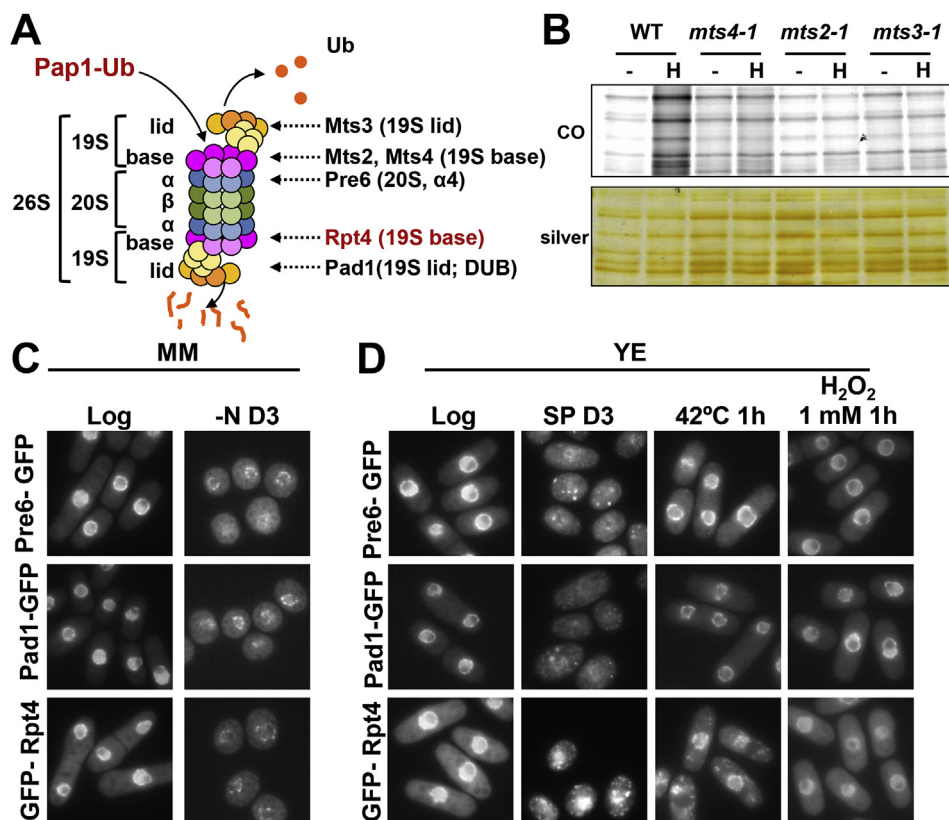
Fig. 3. Defective proteasome subunits enhance tolerance to oxidative stress. (A) Scheme depicting the 26S proteasome structure. (B) Protein carbonyl determination (CO) in extracts from strains 972 (WT), 42.79 (*mts4-1*), 42.80 (*mts2-1*) and 42.81 (*mts3-1*) grown at 30 °C and treated as in Fig. 1A. Silver staining is used as loading control (silver). (C) Fluorescence microscopy of strains expressing GFP-tagged versions of the proteasomal subunits Pre6 (LM98), Pad1 (SB361) and Rpt4 (LM117) in cells growing in MM and in cells subjected to nitrogen starvation for 3 days (-N D3). (D) Fluorescence microscopy of strains described above growing logarithmically in YE, after 3 days in stationary phase (SP D3), subjected to a 42 °C heat shock or to a 1 mM H_2O_2 treatment for 1 h.

degradation even under basal conditions. To confirm it, we measured Pap1 protein levels in a strain lacking the importin Imp1. As shown in Fig. 4B, Pap1 levels are enhanced in this strain background. Furthermore, basal cytosol-to-nucleus shuttling seems to occur even in the absence of the essential cysteine residue C278, required for H_2O_2–dependent disulfide bond formation, since the levels of mutant Pap1.C278A are identical to those of wild-type Pap1 (Fig. 4B), suggesting that the interactions of Pap1 with Imp1 first and with the E3 ligase Ubr1 later does not require oxidation of the transcription factor by peroxides.

We next searched for other domains in Pap1 required for Ubr1-mediated degradation. We generated four GFP-tagged Pap1 derivatives, and expressed them in cells lacking endogenous Pap1. As expected, a mutant protein lacking both the nuclear localization signal (NLS) motif and the basic leucine zipper (bZIP) of the transcription factor cannot be imported to the nucleus after stress imposition (Fig. 4C; Pap1.Δ1), while the protein domain between the NLS-bZIP and the first track of cysteine residues is fully dispensable for protein import (Fig. 4C; Pap1.Δ2) and for protein function (Fig. S3A). Pap1.Δ3, lacking another domain in Pap1 (from residues 84 to 193), is also unable to accumulate at the nucleus upon stress, confirming that this deletion is sufficient to disrupt Pap1 nuclear import (Fig. 4C). As expected, the constitutively cytosolic Pap1.Δ1 and Pap.Δ3 mutants display high protein levels compared to wild-type or Pap1.Δ2 proteins (Fig. 4D).

We generated a mutant lacking residues 101 to 160, which maintains a functional NLS, and therefore accumulates at the nucleus upon stress (Fig. 4C; Pap1.Δ4) but lacks the DNA binding motif. This truncated Pap1 version is still subject to nucleus-to-cytoplasm Crm1-dependent export, since both full length Pap1 and Pap1.Δ4 accumulate in the nucleus upon addition of the Crm1 inhibitor leptomycin B (Fig. S3B). Surprisingly, extracts from cells expressing this mutant display high steady-state levels of the transcription factor, as determined by immunoblot analysis, even though the protein is efficiently imported to the nucleus (Fig. 4D). As shown in Fig. 4E, the basal levels of Pap1.Δ4 are similar to those of full length Pap1 expressed in a *Δubr1*

background, suggesting that this deletion protein is not subject to Ubr1-dependent degradation. As expected, deletion of this domain fully abolishes Pap1.Δ4 binding to stress promoters, as demonstrated with chromatin immuno-precipitation (Fig. 4F), and also protein function (Fig. S3A). To dismiss that DNA binding is required for interaction of the transcription factor with the E3 ligase Ubr1, we analyzed the steady-state levels of a Pap1 mutant, Pap1.GAA [29] (Fig. 4G), which carries three point mutations fully disturbing DNA binding (Fig. 4F) and protein function (Fig. S3A), but not affecting protein import (Fig. S3C). As shown in Fig. 4H, the steady-state levels of Pap1.GAA are as low as those of wild-type Pap1. These experiments suggest that amino acids 101 to 160 of Pap1, which are missing in the Pap1.Δ4 mutant, are required for the interaction of the transcription factor with Ubr1.

2.5. Identification of a 30 amino acid degron in Pap1 subject to Ubr1-dependent regulation

We fused the putative degron of Pap1, expanding residues 101 to 161, as well as two smaller domains of only 30 amino acids each, to GFP and we called them degron 1 (Deg1; residues 102 to 161), Deg2 (residues 102 to 134) and Deg3 (residues 128 to 161) (Fig. 5A). To dismiss protein degradation due to the Ubr11-dependent N-end rule pathway, our three protein chimeras contain a lysine after the first methionine, which has been described to be a stabilizing combination in *S. cerevisiae* [46]; indeed, *Δubr11* cells did not alter protein turnover of the chimeras (Fig. S4A). As shown using fluorescence microscopy, the three GFP-tagged proteins are localized in both the cytosol and the nucleus (Fig. 5B). This dual localization is probably due to direct diffusion through the nuclear pore complex, since they do not accumulate in the nucleus upon leptomycin B treatment (Fig. 5B). As shown in Fig. 5C, the concentration of Deg1-GFP in cell extracts decreased 90–120 min after the addition of the translation inhibitor cycloheximide (CHX), as did the concentration of Deg3-GFP. On the contrary, basal levels of Deg2-GFP or of control GFP are significantly higher than in the other two fusion proteins, and the chimera remains stable upon
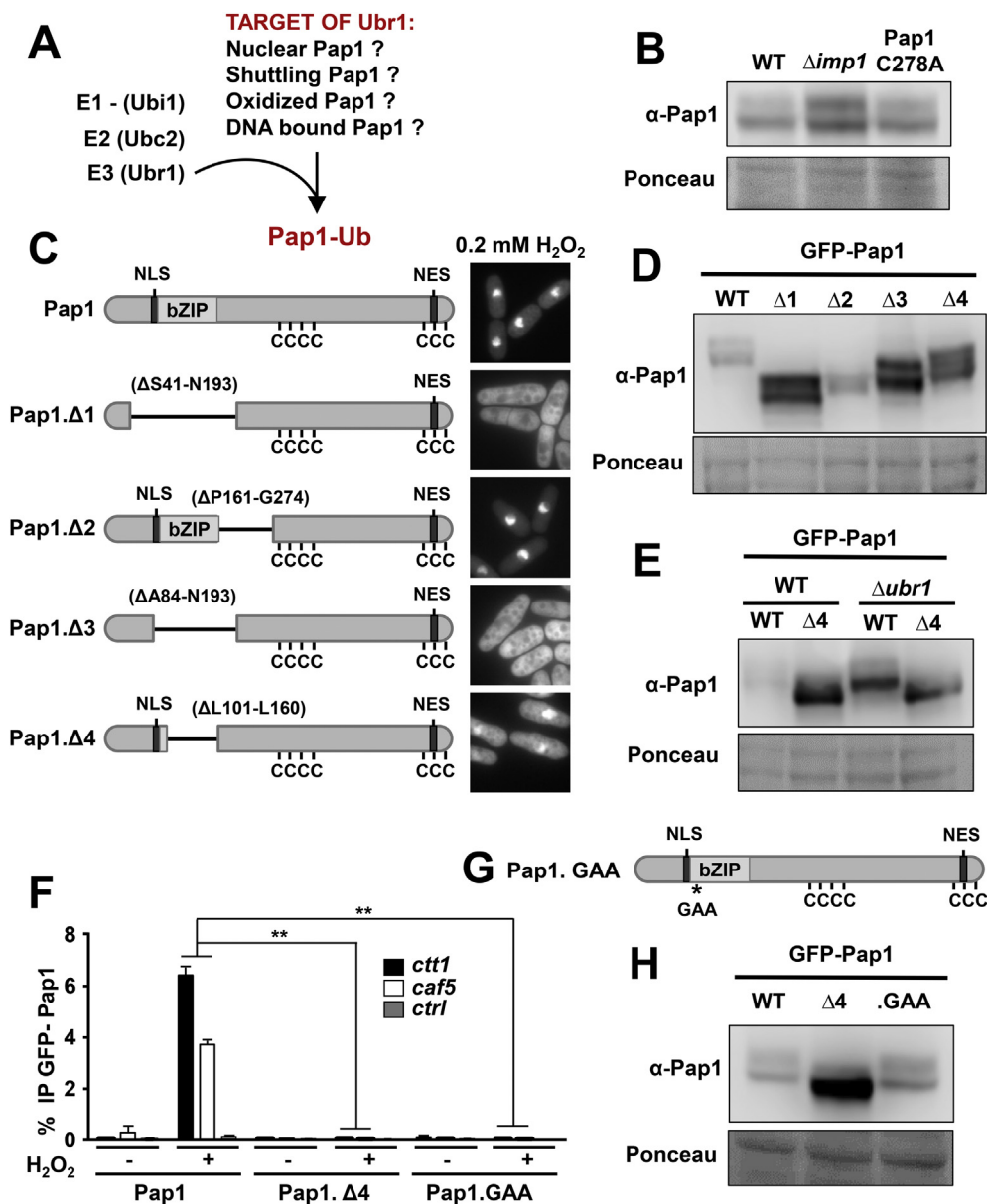
Fig. 4. Cell localization and Pap1 steady state levels. (A) Scheme depicting four possible non-exclusive Pap1 states susceptible to be target of the E3-ligase Ubr1. (B) Steady-state Pap1 levels determined by Western Blot of TCA extracts from 972 (WT), EP150 (Δ*imp1*) and IC2·C278A (Pap1.C78A) strains. Ponceau staining of membranes was used as loading control. (C) Pap1 cellular localization in strains harbouring GFP-Pap1 controlled by the inducible *nmt41x'* promoter and carrying deletions in the Pap1 NLS and b-ZIP regions as shown in the scheme. Strains LM101 (full-length GFP-Pap1), LM101.Δ1 (GFP-Pap1.Δ1), LM101.Δ2 (GFP-Pap1.Δ2), LM101.Δ3, (GFP-Pap1.Δ3) and LM101.Δ4 (GFP-Pap1.Δ4) were treated with 0.2 mM H$_2$O$_2$ for 4 min and Pap1 cell localization determined by fluorescence microscopy. (D) Steady-state Pap1 levels determined by Western Blot of TCA extracts from strains described in C. Ponceau staining of membranes was used as loading control. (E) Steady-state Pap1 levels determined by Western Blot of TCA extracts from strains LM101 (full-length GFP-Pap1), LM101.Δ4 (GFP-Pap1.Δ4), LM37 (full-length GFP-Pap1 Δ*ubr1*) and LM37.Δ4 (GFP-Pap1.Δ4 Δ*ubr1*). Ponceau staining of membranes was used as loading control. (F) Chromatin immuno-precipitation of Pap1 bound to the promoters of the Pap1 dependent genes *ctt1* and *caf5* in strains LM101 (full-length GFP-Pap1), LM101.Δ4 (GFP-Pap1.Δ4) and LM101.GAA (GFP-Pap1.GAA) treated (+) or not (−) with 0.2 mM H$_2$O$_2$ for 5 min. An intergenic region was used as negative control (Ctrl). Error bars (SD) for all ChIP experiments were calculated from three biological triplicates. Significant differences between Pap1 binding to Pap1 dependent genes after stress were determined by the unpaired Student's *t*-test (**P < 0.01). (G) Scheme depicting the localization of the single point mutation GAA in the b-ZIP region of Pap1. (H) Steady-state Pap1 levels determined by Western Blot of TCA extracts from strains LM101, LM101.Δ4 and LM101.GAA. Ponceau staining of membranes was used as loading control.

CHX addition (Fig. 5C). Degradation of Deg3-GFP after CHX addition is fully dependent on Ubr1, whereas the half-life of Deg1-GFP is very similar in wild type and Δ*ubr1* cells (Fig. 5D). Another E3 ligase identified in our screening, SPBC14F5.10c, does not affect the stability of Deg1-GFP (Fig. S4B). On the contrary, the third E3 ligase identified in our screen, Hul5, contributes to the degradation of Deg1-GFP, since cells lacking both Ubr1 and Hul5 are able to significantly stabilize the chimera (Fig. 5E); Hul5 is not required for stabilizing Deg3-GFP (Fig. S4C). In fact, the steady state levels of full length Pap1 are higher in the double mutant Δ*ubr1* Δ*hul5* than in the single individual Δ*ubr1* mutant (Fig. 5F).

3. Discussion

Through a genetic screening of PQC mutants displaying enhanced tolerance to peroxides, we have identified here seven deletion strains, coding for UPS components regulating Pap1 stability (Fig. 5G), which display moderate (two-three fold) up-regulation of steady-state Pap1 levels; this is sufficient to increase wild-type tolerance to H$_2$O$_2$ and to drugs, suggesting that the Pap1-dependent gene expression program can be easily engaged in these backgrounds. Constitutive activation of signal transduction pathways is often deleterious for cell fitness, and the steady-state levels of transcription factors are actively maintained low to avoid hyper-activation of gene programs. For instance, the MAP kinase Sty1 and upstream components respond to high levels of peroxides in fission yeast and to many other signals which compromise cell viability; activated/phosphorylated Sty1 also accumulates at the nucleus upon stress to trigger a massive antioxidant gene expression program. Cells with constitutive activation of the Sty1 cascade, such as those lacking the MAP kinase phosphatase Pyp1 or over-expressing the Sty1 kinase, Wis1, display growth defects [47]. Similarly, constitutive expression of nuclear Pap1 also compromises cell fitness [9]. Therefore, it is not surprising that a complex network related with UPS maintains the levels of the Pap1 transcription factor under a certain threshold.
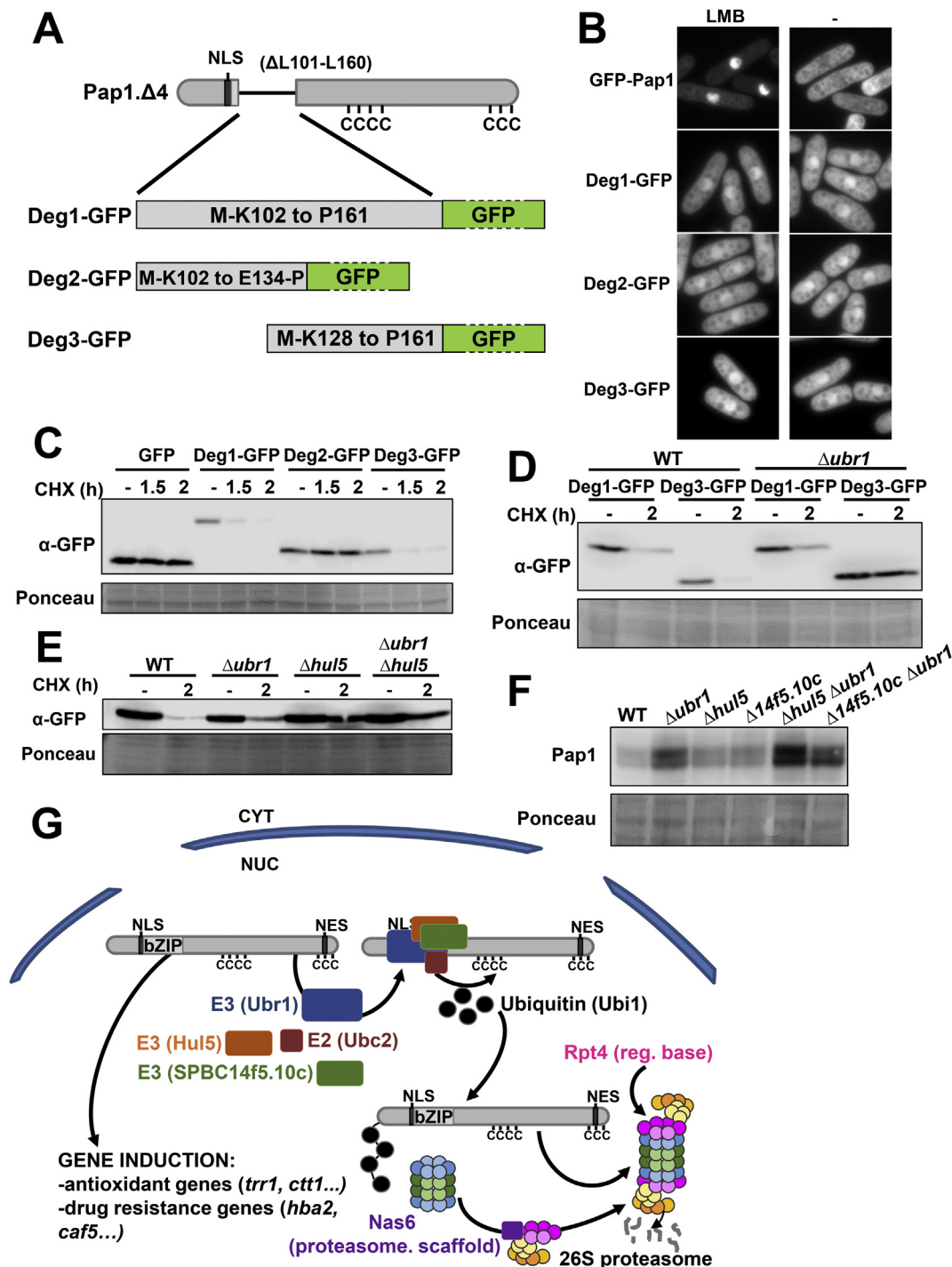
Fig. 5. Identification of Deg3 as a 30 amino acids long, Ubr1-dependent Pap1 degron in Pap1. (A) Scheme depicting the construction of 3 chimeras consisting of small Pap1 domains with putative degron sequences within the b-ZIP region of Pap1 fused to GFP and with a methionine residue in the first position. Degron 1 (Deg1-GFP) encompasses residues from K101 to P161. Degron 2 (Deg 2-GFP) encompasses residues from K102 to E134. Degron 3 (Deg3-GFP) encompasses residues from K128 to P161. Chimeras were expressed under the control of the constitutive *sty1* promoter. (B) Strains LM101 (full-length GFP-Pap1), LM146, (Deg1-GFP), LM147 (Deg2-GFP) and LM148 (Deg3-GFP) were treated or not (−) with 0.1 mM Leptomycin B for 50 min and GFP-Pap1 or GFP-fused degron localization was determined by fluorescence microscopy. (C) Strains LM166 (GFP alone), LM146 (Deg1-GFP), LM147 (Deg2-GFP) and LM148 (Deg3-GFP) were treated with 0.1 mg/ml CHX for 1.5 and 2 h. The GFP-fused degron levels were analyzed by Western Blot of TCA extracts. Ponceau staining is used as loading control. (D) Strains LM146 (Deg1-GFP), LM148 (Deg3-GFP), LM149 (Deg1-GFP *Δubr1*) and LM151 (Deg3-GFP *Δubr1*) were untreated (−) or treated (+) for 2 h with 0.1 mg/ml CHX and analyzed as in B. (E) Strains LM146 (wild type), LM149 (*Δubr1*), LM199 (*Δhul5*), LM195 (*Δubr1 Δhul5*), all expressing Deg1-GFP, were treated and analyzed as in A. (F) Steady state endogenous Pap1 levels from strains 972 (WT), SG282 (*Δubr1*), SB22 (*Δhul5*), LM90 (*ΔSPBC14F5.10c*), LM190 (*Δhul5 Δubr1*) and LM192 (*ΔSPBC14F5.10c Δubr1*) was determined as in Fig. 2F. (G) Scheme depicting a model of Pap1 nuclear degradation that summarizes the involvement of the different components of the UPS identified in this work to have a role in Pap1 degradation.

It has been demonstrated before for Pap1 and for its *S. cerevisiae* ortholog Yap1 that the oxidized transcription factor, bound to DNA, is the target of the Ub-mediated degradation machinery [29,48]. We further show here that, even in the absence of oxidation, the nuclear degradation of the transcription factor Pap1 occurs even in the absence of stress imposition due to cytosol-to-nucleus shuttling, since the Pap1.C278A mutant, lacking a cysteine residue essential for H_2O_2-mediated disulfide formation, is maintained at low steady-state levels, while in cells lacking the Pap1 importin Imp1 promote the accumulation of the transcription factor (Fig. 4B).

Among the eight UPS mutants identified in our screening with dual peroxide and caffeine enhanced tolerance, we have here demonstrated increased Pap1 protein levels in seven of them, except in Δltn1 cells. Ltn1 or listerin in animal cells belongs to the ribosome-associated PQC system, as it binds to 60S ribosomal subunits to ubiquitinate nascent stalled polypeptides, such as aberrant misfolded products [for a review, see Ref. [49]]. Further work will be required to understand the participation of Ltn1 in the regulation of the Pap1 pathway.

Mutations in essential proteasome subunits had been reported to confer multidrug resistance in a Pap1-dependent manner [30]. We have isolated in our screen strain Δrpt4. The non-essential 19S base subunit Rpt4 seems to have a regulation, at least regarding cellular localization, slightly different from other essential proteasome subunits such as Pre6 or Pad1, at least in response to heat shock (Fig. 3D). The only report suggesting that *S. pombe* Rpt4 may have non-proteolytic functions, based on the characterization of some temperature-sensitive mutants in Rpt4 and neighbor subunits, is that it may be involved in the establishment of some boundary elements between heterochromatin and euchromatin to avoid the spreading of the former [39]. But we propose that Rpt4 regulates Pap1 concentration through a standard protease-dependent role, similar to other proteasomal subunits.

As previously reported before, we have demonstrated here that Pap1 is a substrate of the E3 ligase Ubr1. Cells lacking Ubr1 display severe fitness phenotypes (data not shown), and probably other Ubr1 substrates have to be identified. Among them, it has been reported that Ubr1 negatively regulates sexual differentiation in *S. pombe* by degrading the meiotic inducer Mei2 during the mitotic cycle [50], and a 428 amino acid long domain in Mei2 was shown to mediate Ubr1 interaction. Here, we have identified a 30 amino acid peptide as the degron mediating Ubr1-dependent Pap1 degradation, containing two lysine residues, which may be the targets of ubiquitination. Whether a similar domain is present in Mei2 or in other putative Ubr1 substrates is currently under investigation.

4. Materials and methods

4.1. Growth conditions, yeast strains and plasmids

Cells were grown in rich medium (YE) or synthetic minimal medium (MM) as described previously [51]. Origins and genotypes of strains used in this study are outlined in Table S2. Plasmid p419, expressing Ctt1, has been previously described [52]. Tagging of genes was done using homologous recombination with PCR fragments, using as templates pFA6a plasmid derivatives [53]. Most deletions were obtained by crossing deletion mutants from the Bioneer collection [54] with wild type strain 972 to remove auxotrophies. To express GFP-Rpt4, we constructed an integrative plasmid, p711′, to express the chimera under the control of the constitutive *sty1* promoter. Plasmids to obtain strains with GFP-Pap1 under the control of the *nmt41x* promoter and bearing single point Pap1 mutations or deletions in Pap1 domains were derived from plasmid p85.41x' [44]. Plasmid p85.Δ1.41x′, coding for a truncated Pap1 lacking residues S41 to N193, was generated by PCR amplification of the C-terminal-coding domain and cloning into p85.41x′ digested with *Bgl*II and *Sma*I. To obtain plasmid p85.Δ2.41x′, a synthetic fragment of Pap1 ORF (Integrated DNA Technologies, IA, USA) lacking residues from P161 to G274 was cut with *Bgl*II and *Spe*I and

cloned into p85.41x′ digested with the same enzymes. To obtain p85.Δ3.41x′, a PCR fragment of Pap1 ORF lacking residues from A84 to N193 was cut with *Bgl*II and *Nsi*I and cloned into p85.41x′ digested with the same enzymes. To obtain p85.Δ4.41x′, a synthetic fragment of Pap1 ORF lacking residues from L101 to L160 was cut with *Bgl*II and *Nsi*I and cloned into p85.41x′ digested with the same enzymes. To obtain plasmid p85.GAA.41x′, a PCR fragment of Pap1 ORF bearing the single point mutations A89G, Q90G and F93A was obtained using DNA from strain KK2264 [29] as template, cut with *Bgl*II and *Nsi*I and cloned into p85.41x′ digested with the same enzymes. To obtain yeast strains expressing the full-length GFP-Pap1 or the mutant versions, plasmid 85.41x′ and derivatives were linearized with *Nru*I and transformed into strain IC1 [31]. To obtain a plasmid expressing GFP under the control of the *sty1* promoter, we PCR-amplified *GFP* and cloned it under the control of the *sty1* promoter, yielding the integrative plasmid p678'. Plasmids to express degrons with GFP fused at C-terminus were made by digesting synthesized gene fragments coding for the degrons and with an additional ATG codon in the first position (Integrated DNA Technologies, IA, USA) with *Xho*I-*Not*I and cloning them into plasmid p581 digested with *Xho*I-*Not*I which codes for GFP under the control of the *sty1* promoter. Degron 1 encompasses nucleotides 303–483 of Pap1 ORF and cloning into p581 resulted in plasmid p632. Degron 2 encompasses nucleotides 303–402 of Pap1 ORF and cloning into p581 resulted in plasmid p633. Degron 3 encompasses nucleotides 384–483 of Pap1 ORF and cloning into p581 resulted in plasmid p634. To obtain the integrative versions of these plasmids, plasmids p632, p633 and p634 were digested with *Pst*I and *Sac*I and fragments coding for the *sty1* promoter-Degron-GFP-*nmt1* terminator cassette were cloned into p386′ digested with *Pst*I-*Sac*I. The resulting plasmids were p635' (Degron 1), p636' (Degron 2), p637' (Degron 3). All integrative plasmids were linearized with *Nru*I and inserted at the *leu1-32* locus of the corresponding strains.

4.2. Solid sensitivity assay

For survival on solid plates, *S. pombe* strains were grown in YE, diluted and spotted in YE or MM medium agar plates as described previously [28]. The spots were allowed to dry, and the plates were incubated at 30 °C during 2–3 days in the presence or not of 12.5 mM caffeine.

4.3. Growth curves

Yeast cells were grown in YE at 30 °C from an initial OD_{600} of 0.1, using an assay based on automatic measurements of optical densities, as previously described [28].

4.4. Determination of total protein carbonyls

Yeast cells were grown in YE to an OD_{600} of 0.5, at which point they were treated with 2.5 mM H_2O_2 for 4 h. Pellets from 50 ml cultures were washed with H_2O, resuspended in carbonylation buffer (8 M urea, 20 mM Na-phosphate buffer pH 6, 1 mM EDTA and protease inhibitors) and lysed by vortexing during 5 min. Protein extracts were incubated with 1% streptomycin sulfate (Sigma, S6501) in ice for 5 min and centrifuged for 5 min. Supernatants were recovered and protein concentration was calculated by Bradford assay and diluted to 1 μg/μl with carbonylation buffer. 100 μg of protein were incubated with 4 μl 50 mM fluorescein 5-thiosemicarbazide (FTC) (Sigma) at 37 °C for 2 h protected from light. Proteins were then precipitated with 10% trichloroacetic acid (TCA), incubated at −20 °C for 10 min and centrifuged 10 min. Pellets were washed three times with chilled ethanol:ethyl acetate (1:1) and let to air dry. To visualize protein carbonyls by sodium dodecyl sulfate-polyacrylamide electrophoresis (SDS-PAGE), pellets were resuspended in 50 μl dilution buffer (8 M urea, 20 mM Na-phosphate buffer pH 8, 1 mM EDTA). Protein concentration

was determined by Bradford assay. 5 μg of protein were loaded with 5-fold sample buffer without any dye. Gels were scanned using Typhoon 8600 Variable Mode Imager scanner (Molecular Dynamics) with a 526 nm short pass filter at 800 V. Gels were then fixed and total protein was visualized by silver staining. Where indicated, protein carbonyl levels were quantified using the ImageQuant 5.2 program (GE healthcare, Little Chalfont, Buckinghamshire, United Kingdom) for carbonyls and ImageJ software for total protein.

4.5. Flow cytometry

Yeast cells were grown in MM to an OD_{600} of 0.5, at which point they were diluted to 0.1. Then cells were sonicated in a 250 Branson Digital Sonifier with 3 ON/OFF 0.5 s and 10% amplitude pulses. The acquisition was performed with a BD FACSCanto™ flow cytometer using tube acquisition. To measure GFP, it was excited at 488 nm and detected using a 530/30 band-pass and 502 LP emission filter. Population of interest was obtained by hierarchical gating using i) forward (FSC) and side (SSC) light scattering, ii) FSC-A against FSC-H to exclude debris and cell clumps and iii) FITC-A and PerCP-Cy5-5-A. 10,000 events were recorded for each sample at medium speed. Data acquisition and processing was performed with BD FACSDiva Software 6.0. GFP/FSC (FITC/FSC) ratio for each sample was calculated with the median values of the final gate (iii) of the final gated population.

4.6. Fluorescence microscopy

Yeast cells were grown in MM to an OD_{600} of 0.5, at which point they were harvested by centrifugation 1 min at 3000 rpm and visualized at room temperature. Images were acquired using a Nikon Eclipse 90i microscope equipped with differential interference contrast optics, a PLAN APO VC 100×1.4 oil immersion objective, an ORCA–II–ERG camera (Hamamatsu), excitation and emission filters GFP-4050B and image acquisition software Metamorph 7.8.13 (Gataca Systems). Processing of all images was performed using Fiji (ImageJ, National Institutes of Health) [55].

4.7. Chromatin immuno-precipitation

To test the binding of Pap1 to promoters, the indicated strains were grown in MM, and chromatin isolation and immuno-precipitation was performed as described [31].

4.8. TCA extracts and Western Blot

TCA extracts to analyze levels of Pap1 and GFP-fused degrons were prepared as described before [45]. Pap1 was visualized with a specific Pap1 antibody or with the JL-8 antibody against GFP (Takara). Protein loading was determined by staining membranes with ATX Ponceau S (Sigma-Aldrich). Briefly, membranes were incubated for 15–30 min in a 1:5 dilution of Ponceau:H_2O, and thoroughly rinsed with H_2O.

Acknowledgements

We thank Sergio Moreno for providing strains.

Appendix A. Supplementary data

Supplementary data to this article can be found online at https://doi.org/10.1016/j.redox.2019.101305.

References

[1] N. Kuksal, J. Chalker, R.J. Mailloux, Progress in understanding the molecular oxygen paradox - function of mitochondrial reactive oxygen species in cell signaling, Biol. Chem. 398 (11) (2017) 1209–1227.

[2] B. Kalyanaraman, Teaching the basics of redox biology to medical and graduate students: oxidants, antioxidants and disease mechanisms, Redox Biol. 1 (2013) 244–257.

[3] S. Fourquet, R. Guerois, D. Biard, M.B. Toledano, Activation of NRF2 by nitrosative agents and H2O2 involves KEAP1 disulfide formation, J. Biol. Chem. 285 (11) (2010) 8463–8471.

[4] H. Sies, C. Berndt, D.P. Jones, Oxidative stress, Annu. Rev. Biochem. 86 (2017) 715–748.

[5] F. Antunes, P.M. Brito, Quantitative biology of hydrogen peroxide signaling, Redox Biol. 13 (2017) 1–7.

[6] S. Stocker, K. Van Laer, A. Mijuskovic, T.P. Dick, The Conundrum of Hydrogen Peroxide Signaling and the Emerging Role of Peroxiredoxins as Redox Relay Hubs, Antioxid Redox Signal, 2017.

[7] H. Sies, Hydrogen peroxide as a central redox signaling molecule in physiological oxidative stress: oxidative eustress, Redox Biol. 11 (2017) 613–619.

[8] H. Tatebe, K. Shiozaki, Identification of Cdc37 as a novel regulator of the stress-responsive mitogen-activated protein kinase, Mol. Cell. Biol. 23 (15) (2003) 5132–5142.

[9] E.A. Castillo, A.P. Vivancos, N. Jones, J. Ayte, E. Hidalgo, Schizosaccharomyces pombe cells lacking the Ran-binding protein Hba1 show a multidrug resistance phenotype due to constitutive nuclear accumulation of Pap1, J. Biol. Chem. 278 (42) (2003) 40565–40572.

[10] J.A. Imlay, Cellular defenses against superoxide and hydrogen peroxide, Annu. Rev. Biochem. 77 (2008) 755–776.

[11] D. Chen, W.M. Toone, J. Mata, R. Lyne, G. Burns, K. Kivinen, A. Brazma, N. Jones, J. Bahler, Global transcriptional responses of fission yeast to environmental stress, Mol. Biol. Cell 14 (1) (2003) 214–229.

[12] D. Chen, C.R. Wilkinson, S. Watt, C.J. Penkett, W.M. Toone, N. Jones, J. Bahler, Multiple pathways differentially regulate global oxidative stress responses in fission yeast, Mol. Biol. Cell 19 (1) (2008) 308–317.

[13] E.R. Stadtman, R.L. Levine, Protein oxidation, Ann. N. Y. Acad. Sci. 899 (2000) 191–208.

[14] B. McDonagh, Detection of ROS induced proteomic signatures by mass spectrometry, Front. Physiol. 8 (2017) 470.

[15] E. Cabiscol, J. Tamarit, J. Ros, Protein carbonylation: proteomics, specificity and relevance to aging, Mass Spectrom. Rev. 33 (1) (2014) 21–48.

[16] E.R. Stadtman, B.S. Berlett, Reactive oxygen-mediated protein oxidation in aging and disease, Drug Metab. Rev. 30 (2) (1998) 225–243.

[17] E.R. Stadtman, Protein oxidation and aging, Free Radic. Res. 40 (12) (2006) 1250–1258.

[18] J. Tyedmers, A. Mogk, B. Bukau, Cellular strategies for controlling protein aggregation, Nat. Rev. Mol. Cell Biol. 11 (11) (2010) 777–788.

[19] Y. Shibata, R.I. Morimoto, How the nucleus copes with proteotoxic stress, Curr. Biol. 24 (10) (2014) R463–R474.

[20] D. Balchin, M. Hayer-Hartl, F.U. Hartl, In vivo aspects of protein folding and quality control, Science 353 (6294) (2016) aac4354.

[21] E.M. Sontag, R.S. Samant, J. Frydman, Mechanisms and functions of spatial protein quality control, Annu. Rev. Biochem. 86 (2017) 97–122.

[22] E. Herrero, J. Ros, G. Belli, E. Cabiscol, Redox control and oxidative stress in yeast cells, Biochim. Biophys. Acta 1780 (11) (2008) 1217–1235.

[23] S. Boronat, A. Domenech, E. Paulo, I.A. Calvo, S. Garcia-Santamarina, P. Garcia, J. Encinar Del Dedo, A. Barcons, E. Serrano, M. Carmona, E. Hidalgo, Thiol-based H2O2 signalling in microbial systems, Redox Biol. 2 (2014) 395–399.

[24] A.P. Vivancos, M. Jara, A. Zuin, M. Sanso, E. Hidalgo, Oxidative stress in Schizosaccharomyces pombe: different H2O2 levels, different response pathways, Mol. Genet. Genom. 276 (6) (2006) 495–502.

[25] T. Toda, M. Shimanuki, M. Yanagida, Fission yeast genes that confer resistance to staurosporine encode an AP-1-like transcription factor and a protein kinase related to the mammalian ERK1/MAP2 and budding yeast FUS3 and KSS1 kinases, Genes Dev. 5 (1) (1991) 60–73.

[26] T.G. Turi, P. Webster, J.K. Rose, Brefeldin A sensitivity and resistance in Schizosaccharomyces pombe. Isolation of multiple genes conferring resistance, J. Biol. Chem. 269 (39) (1994) 24229–24236.

[27] Z. Benko, C. Fenyvesvolgyi, M. Pesti, M. Sipiczki, The transcription factor Pap1/Caf3 plays a central role in the determination of caffeine resistance in Schizosaccharomyces pombe, Mol. Genet. Genom. 271 (2) (2004) 161–170.

[28] I.A. Calvo, N. Gabrielli, I. Iglesias-Baena, S. Garcia-Santamarina, K.L. Hoe, D.U. Kim, M. Sanso, A. Zuin, P. Perez, J. Ayte, E. Hidalgo, Genome-wide screen of genes required for caffeine tolerance in fission yeast, PLoS One 4 (8) (2009) e6619.

[29] K. Kitamura, M. Taki, N. Tanaka, I. Yamashita, Fission yeast Ubr1 ubiquitin ligase influences the oxidative stress response via degradation of active Pap1 bZIP transcription factor in the nucleus, Mol. Microbiol. 80 (3) (2011) 739–755.

[30] M. Penney, I. Samejima, C.R. Wilkinson, C.J. McInerny, S.G. Mathiassen, M. Wallace, T. Toda, R. Hartmann-Petersen, C. Gordon, Fission yeast 26S

proteasome mutants are multi-drug resistant due to stabilization of the Pap1 transcription factor, PLoS One 7 (11) (2012) e50796.

[31] I.A. Calvo, P. Garcia, J. Ayte, E. Hidalgo, The transcription factors Pap1 and Prr1 collaborate to activate antioxidant, but not drug tolerance, genes in response to H2O2, Nucleic Acids Res. 40 (11) (2012) 4816–4824.

[32] W.M. Toone, S. Kuge, M. Samuels, B.A. Morgan, T. Toda, N. Jones, Regulation of the fission yeast transcription factor Pap1 by oxidative stress: requirement for the nuclear export factor Crm1 (Exportin) and the stress-activated MAP kinase Sty1/Spc1 [published erratum appears in Genes Dev 1998 Aug 15;12(16):2650] [see comments], Genes Dev. 12 (10) (1998) 1453–1463.

[33] N. Kudo, H. Taoka, T. Toda, M. Yoshida, S. Horinouchi, A novel nuclear export signal sensitive to oxidative stress in the fission yeast transcription factor Pap1, J. Biol. Chem. 274 (21) (1999) 15151–15158.

[34] I.A. Calvo, S. Boronat, A. Domenech, S. Garcia-Santamarina, J. Ayte, E. Hidalgo, Dissection of a redox relay: H2O2-dependent activation of the transcription factor Pap1 through the peroxidatic Tpx1-thioredoxin cycle, Cell Rep. 5 (5) (2013) 1413–1424.

[35] M. Shimanuki, Y. Saka, M. Yanagida, T. Toda, A novel essential fission yeast gene pad1+ positively regulates pap1(+)-dependent transcription and is implicated in the maintenance of chromosome structure, J. Cell Sci. 108 (Pt 2) (1995) 569–579.

[36] V. Spataro, T. Toda, R. Craig, M. Seeger, W. Dubiel, A.L. Harris, C. Norbury, Resistance to diverse drugs and ultraviolet light conferred by overexpression of a novel human 26 S proteasome subunit, J. Biol. Chem. 272 (48) (1997) 30470–30475.

[37] F. Li, G. Tian, D. Langager, V. Sokolova, D. Finley, S. Park, Nucleotide-dependent switch in proteasome assembly mediated by the Nas6 chaperone, Proc. Natl. Acad. Sci. U. S. A. 114 (7) (2017) 1548–1553.

[38] S. Bohn, F. Beck, E. Sakata, T. Walzthoeni, M. Beck, R. Aebersold, F. Forster, W. Baumeister, S. Nickell, Structure of the 26S proteasome from Schizosaccharomyces pombe at subnanometer resolution, Proc. Natl. Acad. Sci. U. S. A. 107 (49) (2010) 20992–20997.

[39] H.D. Seo, Y. Choi, M. Kim, K. Kang, T. Urano, D. Lee, The 19S proteasome is directly involved in the regulation of heterochromatin spreading in fission yeast, J. Biol. Chem. 292 (41) (2017) 17144–17155.

[40] C.R. Wilkinson, M. Wallace, M. Morphew, P. Perry, R. Allshire, J.P. Javerzat, J.R. McIntosh, C. Gordon, Localization of the 26S proteasome during mitosis and meiosis in fission yeast, EMBO J. 17 (22) (1998) 6465–6476.

[41] K. Takeda, T. Yoshida, S. Kikuchi, K. Nagao, A. Kokubu, T. Pluskal, A. Villar-Briones, T. Nakamura, M. Yanagida, Synergistic roles of the proteasome and autophagy for mitochondrial maintenance and chronological lifespan in fission yeast, Proc. Natl. Acad. Sci. U. S. A. 107 (8) (2010) 3540–3545.

[42] H. Fujiwara, N. Tanaka, I. Yamashita, K. Kitamura, Essential role of Ubr11, but not Ubr1, as an N-end rule ubiquitin ligase in Schizosaccharomyces pombe, Yeast 30 (1) (2013) 1–11.

[43] M. Umeda, S. Izaddoost, I. Cushman, M.S. Moore, S. Sazer, The fission yeast Schizosaccharomyces pombe has two importin-alpha proteins, Imp1p and Cut15p, which have common and unique functions in nucleocytoplasmic transport and cell cycle progression, Genetics 171 (1) (2005) 7–21.

[44] E.A. Castillo, J. Ayte, C. Chiva, A. Moldon, M. Carrascal, J. Abian, N. Jones, E. Hidalgo, Diethylmaleate activates the transcription factor Pap1 by covalent modification of critical cysteine residues, Mol. Microbiol. 45 (1) (2002) 243–254.

[45] A.P. Vivancos, E.A. Castillo, B. Biteau, C. Nicot, J. Ayte, M.B. Toledano, E. Hidalgo, A cysteine-sulfinic acid in peroxiredoxin regulates H2O2-sensing by the antioxidant Pap1 pathway, Proc. Natl. Acad. Sci. U. S. A. 102 (25) (2005) 8875–8880.

[46] C.S. Hwang, A. Shemorry, A. Varshavsky, N-terminal acetylation of cellular proteins creates specific degradation signals, Science 327 (5968) (2010) 973–977.

[47] K. Shiozaki, P. Russell, Cell-cycle control linked to extracellular environment by MAP kinase pathway in fission yeast, Nature 378 (6558) (1995) 739–743.

[48] K. Gulshan, B. Thommandru, W.S. Moye-Rowley, Proteolytic degradation of the Yap1 transcription factor is regulated by subcellular localization and the E3 ubiquitin ligase Not4, J. Biol. Chem. 287 (32) (2012) 26796–26805.

[49] C.A.P. Joazeiro, Ribosomal stalling during translation: providing substrates for ribosome-associated protein quality control, Annu. Rev. Cell Dev. Biol. 33 (2017) 343–368.

[50] K. Kitamura, S. Katayama, S. Dhut, M. Sato, Y. Watanabe, M. Yamamoto, T. Toda, Phosphorylation of Mei2 and Ste11 by Pat1 kinase inhibits sexual differentiation via ubiquitin proteolysis and 14-3-3 protein in fission yeast, Dev. Cell 1 (3) (2001) 389–399.

[51] C. Alfa, P. Fantes, J. Hyams, M. McLeod, E. Warbrick, Experiments with Fission Yeast: A Laboratory Course Manual, Cold Spring Harbor Laboratory, Cold Spring Harbor, N.Y., 1993.

[52] E. Paulo, S. Garcia-Santamarina, I.A. Calvo, M. Carmona, S. Boronat, A. Domenech, J. Ayte, E. Hidalgo, A genetic approach to study H2O2 scavenging in fission yeast– distinct roles of peroxiredoxin and catalase, Mol. Microbiol. 92 (2) (2014) 246–257.

[53] J. Bahler, J.Q. Wu, M.S. Longtine, N.G. Shah, A. McKenzie III, A.B. Steever, A. Wach, P. Philippsen, J.R. Pringle, Heterologous modules for efficient and versatile PCR-based gene targeting in Schizosaccharomyces pombe, Yeast 14 (10) (1998) 943–951.

[54] D.U. Kim, J. Hayles, D. Kim, V. Wood, H.O. Park, M. Won, H.S. Yoo, T. Duhig, M. Nam, G. Palmer, S. Han, L. Jeffery, S.T. Baek, H. Lee, Y.S. Shim, M. Lee, L. Kim, K.S. Heo, E.J. Noh, A.R. Lee, Y.J. Jang, K.S. Chung, S.J. Choi, J.Y. Park, Y. Park, H.M. Kim, S.K. Park, H.J. Park, E.J. Kang, H.B. Kim, H.S. Kang, H.M. Park, K. Kim, K. Song, K.B. Song, P. Nurse, K.L. Hoe, Analysis of a genome-wide set of gene deletions in the fission yeast Schizosaccharomyces pombe, Nat. Biotechnol. 28 (6) (2010) 617–623.

[55] J. Schindelin, I. Arganda-Carreras, E. Frise, V. Kaynig, M. Longair, T. Pietzsch, S. Preibisch, C. Rueden, S. Saalfeld, B. Schmid, J.Y. Tinevez, D.J. White, V. Hartenstein, K. Eliceiri, P. Tomancak, A. Cardona, Fiji: an open-source platform for biological-image analysis, Nat. Methods 9 (7) (2012) 676–682.